Journal of the Korean Society of Oceanography
Vol. 39, No. 1, pp. 46 — 56 March 2004

Measuring and Modeling the Spectral Attenuation of Light in the Yellow Sea

SONIA C. GALLEGOS[1]*, JUANITA SANDIDGE[1], XIAOGANG CHEN[2], SANGBOK D. HAHN[3], YU-HWAN AHN[4], RODOLFO ITURRIAGA[5], HEE DONG JEONG[6], YOUNG SANG SUH[6] AND SUNGHWAM CHO[3]

[1]*Naval Research Laboratory, Oceanography Division. MS 39529 - U.S.A.*
[2]*Planning Systems Inc., Stennis Space Center, MS 39529 USA*
[3]*West Fisheries Research and Development Institute, Jung-gu Buksung-dong 1ga, 98-36400-201 Inchon, Korea*
[4]*Korean Ocean Research and Development Institute, Ansan P.O. Box 29, Seoul 425-600 Korea*
[5]*University of Southern California, Wrigley Institute for Environmental Sciences, Los Angeles, California 90089-USA*
[6]*National Fisheries Reseach and Development Institute, 408-1 Shirang-Ri, Kuang-Up, Kijang-Gun, Pusan Korea 619-900*

Spectral attenuation of light and upwelling radiance were measured in the western coast of Korea on board the R/V Inchon 888 of the Korean National Fisheries Research and Development Institute (NFRDI) during four seasons. The goal of these efforts was to determine the spatial and temporal distribution of the inherent and apparent optical properties of the water, and the factors that control their distribution. Our data indicate that while stratification of the water column, phytoplankton, and wind stress determined the vertical distribution of the optical parameters offshore, it was the tidal current and sediment type that controlled both the vertical and horizontal distribution in the coastal areas. These findings led to the development of a model that estimates the spectral attenuation of light with respect to depth and time for the Yellow Sea. The model integrates water leaving radiance from satellites, sediment types, current vectors, sigma-t, bathymetry, and *in situ* optical measurements in a learning algorithm capable of extracting optical properties with only knowledge of the environmental conditions of the Yellow Sea. The performance of the model decreases with increase in depth. The mean absolute percentage error (MAPE) of the model is 2% for the upper five meters, 8-10% between 6 and 50 meters, and 15% below 51 meters.

Key words: Yellow Sea, Attenuation

INTRODUCTION

The Yellow Sea is a semi-enclosed shallow basin with depths less than 100 m. The attenuation of light of its waters is controlled by factors such as strong tidal currents, the stirring action of the wind, coastal runoff, sediment distributions, phytoplankton blooms, and stratification of the water column. In general, minimum transparency occurs in the winter and maximum transparency in the summer and early fall (Hahn, 1968; Choi and Shim, 1986; Zhu and Zhao, 1991). In the winter, strong winds resuspend large amounts of particulate matter into the water column contributing to the decrease in light attenuation. This is particularly true of the coast of China which experiences changes in sea surface heights (SSH) of up to 20 cm due to winter northerly and southerly bursts of wind that have a time scale of a few days. The changes in SSH gives rise to coastal shelf waves that propagate south along the coasts of China with speeds of about 12 m/s (Jacobs *et al.*, 1998). The maximum transparency observed in the summer and early fall is the result of a stable water column induced by a persistent thermocline. Monsoons and subsequent increase in rainfall contribute to the increase in particle load from river outflows and changes in transparency (Wells, 1988). Phytoplankton blooms present at the onset of the spring bloom contribute to the decrease in transparency in the upper layers of the water during the spring months (Fei, 1986).

Tidal currents control the distribution and variability of the water properties, including attenuation in the Yellow Sea throughout the seasons. Tidal range in the Yellow Sea is over 2 m, and maximum current velocities are between 50 and 80 cm/s (Teague *et al.*, 1998). Mean currents after tidal components are

*Corresponding author: gallegos@nrlssc.navy.mil

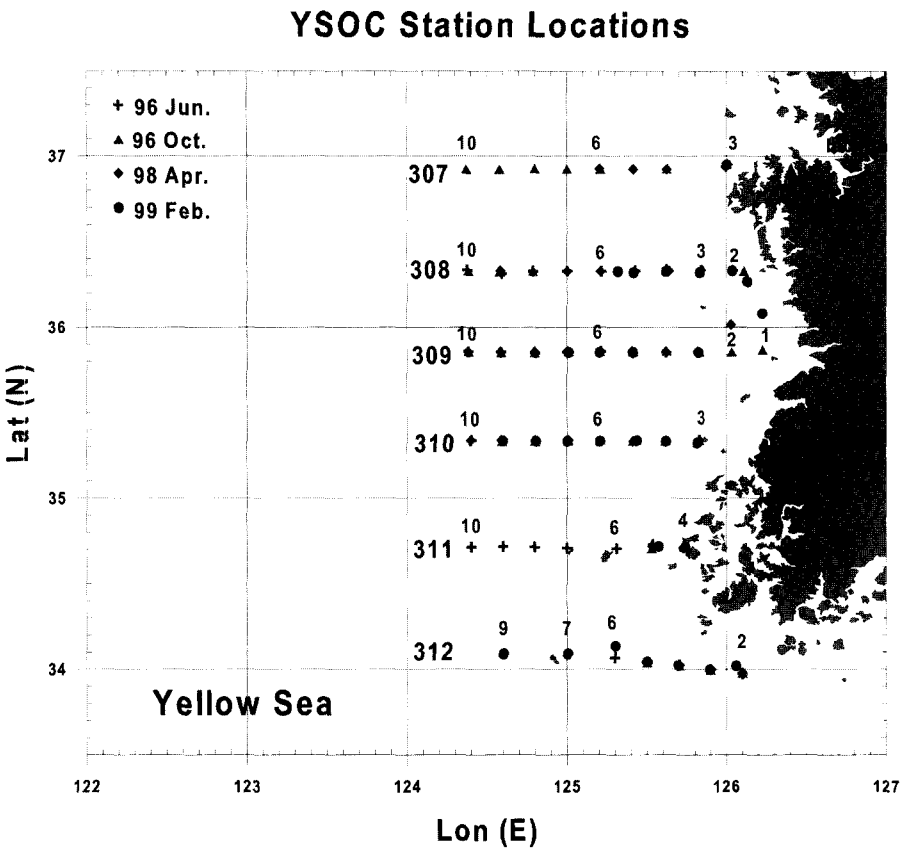

Fig. 1. Location of the *in situ* measurements off the Korean coast.

removed are only 2 to 6 cm/s (Grabber *et al.*, 1989). M2 is the dominant component, followed by S2, and K. Tidal ranges are reported to be up to 6 m in the west coast of Korea (Kang *et al.*, 1991). Tidal range in the middle of the Yellow Sea is greater than 2 m. Tides are found to account for at least 85% of the SSH variance in the Yellow Sea interior (Choi, 1988; Pistek *et al.*, 1998; Teague *et al.*, 1998).

The attenuation of light in the Yellow Sea waters has been linked to sediments and bathymetry (Zhang, 1983), suspended particles (Hahn, 1968; Ahn, 1999), and light penetration (Yang, 1992; Choi and Shim, 1986; Zhu and Zhao, 1991). Winter and summer oceanographic conditions in the Yellow Sea produce different sedimentological regimes (Milliman *et al.*, 1986) and consequently different transparency regimes. While most of the relic sediments in the Yellow Sea come from erosion of the Yellow River sediments, those off the Korean Peninsula are augmented by silts and clays introduced by the Han, Kum and Yalu rivers, which feed extensive tidal mud flats (Wells, 1988). The silts and clays off the Chinese coasts are likely the result of the fine grain sediments from the Changjian River. The sediments are dispersed via surface waves in offshore waters and tidal forcing in the shallower areas (Grabber *et al.*, 1989). The distribution of suspended matter in the Yellow Sea has been addressed by Ahn (1999).

In this paper, we describe efforts to measure spectral attenuation of light (transparency) with respect to depth off the Korean coast and the central Yellow Sea to understand how the attenuation of light changes with respect to depth, time and season. Relying on previous work on water transparency of this area, we also investigate the factors that appear to control the transparency of these waters. Our investigation culminates with an effort to model the attenuation of light for the entire Yellow Sea. We discuss the model and present statistical proof of its accuracy.

METHODS

The goal of our investigation was to quantify the seasonal distribution of inherent and apparent optical properties of the water with respect to depth and season in the Yellow Sea. With this goal in mind, we carried out four cruises during the summer and fall 1996, the spring 1998 and the winter 1999. The area where the optical measurements were obtained appears in Fig. 1. This area is the same area as that of NFRDI

serial stations.

Profiles of upwelling radiance were collected using a profiling radiometer from Satlantic, Inc. of Canada, and spectral attenuation coefficient using an absorption and attenuation sensor (AC-9) from Wetlabs of Oregon, USA. The upwelling radiance profiles were acquired at seven wavelengths (411 nm, 442 nm, 490 nm, 509 nm, 555 nm, 589 nm, and 685 nm). The spectral attenuation profiles were acquired at nine wavelengths (412 nm, 440 nm, 488 nm, 510 nm, 532 nm, 555 nm, 650 nm, 676 nm, and 715 nm). In addition, remote sensing reflectance between 400 nm and 700 nm was measured with a field radiometer from Analytical Spectral Devices (ASD) from Colorado, USA. The measurements were obtained concurrently with CTD measurements by NFRDI. The data were corrected and calibrated according to manufacturers instructions and procedures developed at the Naval Research Laboratory (NRL) at Stennis Space Center in Mississippi, USA. Large spikes corresponding to bubbles and excess data introduced at the time of instrument deployment were removed from the data, and the corrected and calibrated profiles were stored and analyzed.

Temperature, salinity, depth, bathymetry, sediment type, SSH, current speed and direction were computed at the location of each of the optical stations. The temperature salinity and depth profiles came from the NFRDI CTD measurements. The bathymetry for each station was obtained from the ship and *in situ* instrument depth sensors. Sediment type was analyzed from samples collected on board of the R/V Inchon 888 and approximated from a database provided by the Naval Oceanographic Office. Current vectors and SSH were computed for the entire tidal cycle at each specific station using an Adjoint tidal model for the Yellow Sea (AYSTM) (Pistek *et al.*, 1998). A large database containing the optical and environmental parameters per depth and station was constructed and analyzed. Multiple correlations were run on the data in an effort to identify relationships existing among the parameters. Minimum and maximum values of spectral attenuation, and depth corresponding to each of these values were calculated. 3-D plots of spectral attenuation were constructed at various depth intervals to assess the spatial extent of the distributions. Examples of the 3-D attenuation plots are presented in Figs. 2a through 2d.

The *in situ* database consisted of optical measurements of spectral light attenuation, current speed and direction, water density, sediment type and bathymetry. These parameters were used in developing a neural network model and to train its supervised backpropagation learning algorithm. It relies on a gradient descent search technique to minimize the mean squared error between the desired output patterns and the neural network value. The result is a network that produces least square estimates of attenuation with respect to depth and time. The challenging part of developing a neural network based model on limited data such as ours is to find the right combination of inputs, weights, and iterations that would allow the model to "generalize" and produce accurate results without memorization of the data. In the Yellow Sea Optical Model (YSOM), depicted in Fig. 3, we needed a minimum of 28 inputs, one hidden node and an output node. The inputs were a combination of all the oceanographic and geological parameters that were computed or measured in the Yellow Sea. Evaluation of the performance of the weighted inputs in relation to the desired output pattern was carried out with a hyperbolic tangent function. The model was trained with *in situ* data to 60 m, exclusively because our data showed that the tidal effects on the optical properties were clearly observed in the shallower waters. 60 m was an arbitrary depth that included most of the resuspension areas observed in the Sea-viewing Wide Field-of-view Sonsor (SeaWiFS) and Moderate Resolution Imaging Spectral Radiometer (MODIS) imagery. No efforts were invested in training the model below this depth.

Real-time estimation of attenuation coefficient with respect to depth and time is carried out with inputs from NRL oceanographic and coastal models. Temperature and salinity come from the NRL Modular Ocean Data Assimilation System (MODAS), which produces three-dimensional grids of temperature and salinity by combining climatological information with SSH from TOPEX/ERS-2, and Sea Surface Temperature (SST) from the NOAA-Advanced Very High Resolution Radiometer (AVHRR) and local X-BT data (Fox *et al.*, 2002). Currents, SSH and bathymetry come from the AYSTM. Sediment type is obtained from a large database of sediments archived by the Naval Oceanographic Office in the USA. Water leaving radiance is calculated from SeaWiFS or MODIS.

The neural network model produces estimates of spectral attenuation coefficient at 532 nm with a spatial horizontal resolution of 0.05° and a vertical resolution of 5 m from the surface to the bottom of the Yellow Sea. The model can be trained at any

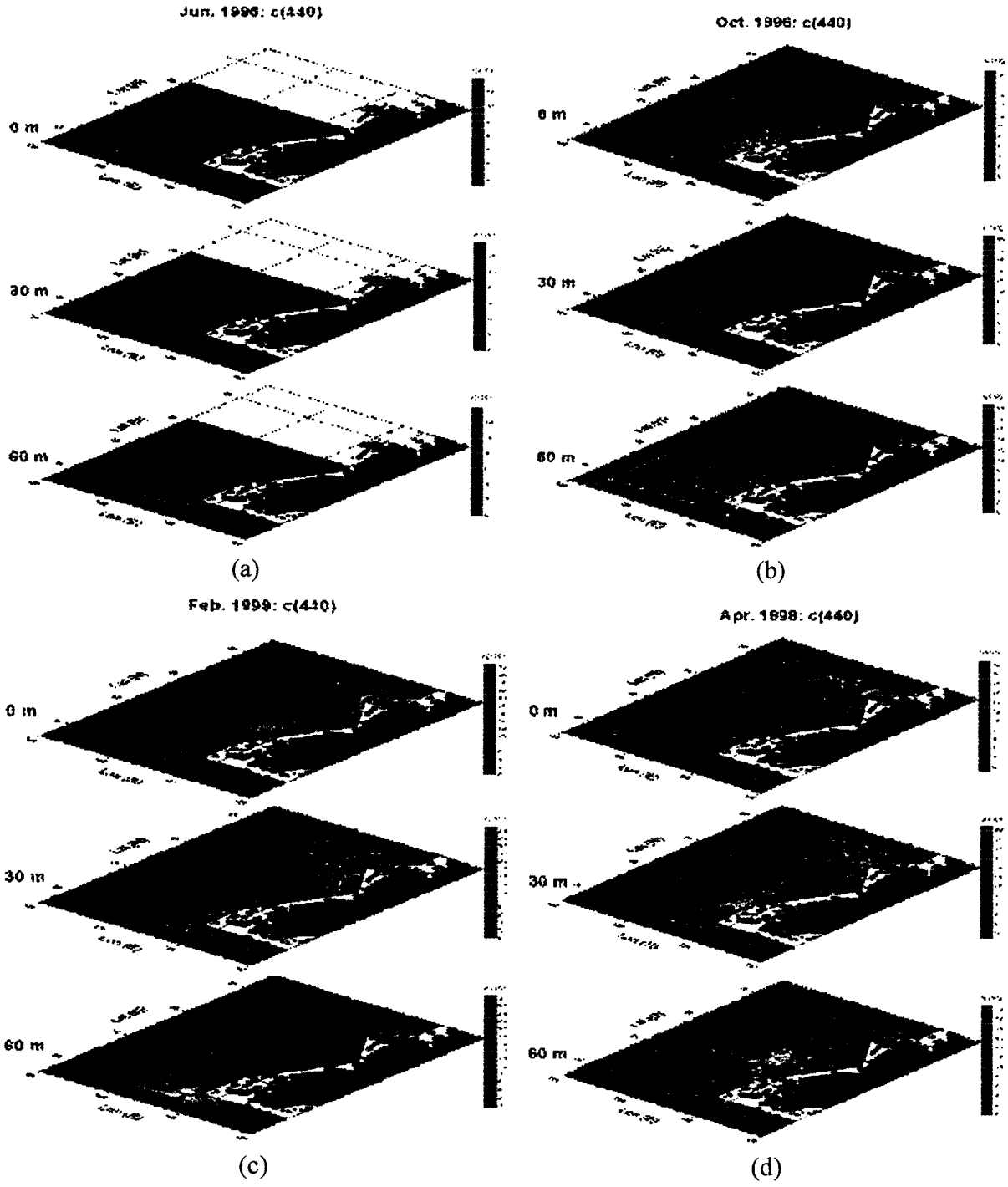

Fig. 2. (a) Measured spectral attenuation for June 1996, (b) Measured spectral attenuation for October 1996, (c) Measured spectral attenuation for February 1999, (d) Measured spectral attenuation for April 1998.

wavelength. We choose to train it at 532 nm because it is within the range of wavelengths of minimum absorption by phytoplankton and detritus. The model is designed to estimate attenuation at hourly intervals. It can operate with and without satellite data. If cloud-free data from SeaWiFS or MODIS is available, the model will use them in the computation of its estimates. If not, the model relies for its estimates on the geophysical parameters, exclusively. This particular capability was added to the model because of the extreme cloudiness and fog typical of the Yellow Sea. Rough estimates of cloud cover in satellite

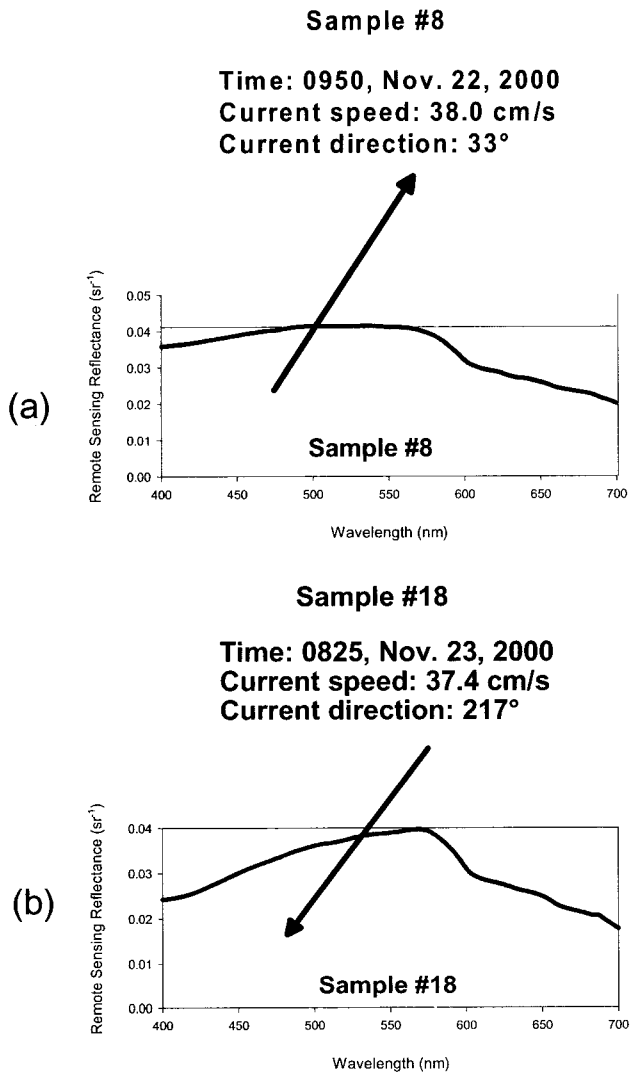

Fig. 3. Architecture of the Yellow Sea Optical Model.

data from the Yellow Sea conducted by the authors, indicate that the Yellow Sea surface is obscured by clouds or fog 68% to 75% of the time depending on the season.

OBSERVATIONS AND RESULTS OF THE FIELD COLLECTIONS

The minimum values of spectral attenuation or the clearest waters in the Yellow Sea occurred in early October. Attenuation decreased in June followed by April. February had the maximum values or the most opaque waters of all the sampled months. These results corroborated previous seasonal trends reported by Hahn (1968), Choi and Shim (1986). To compare the attenuation of light in the various seasons in this study, we used 440 nm. In general, the attenuation at other wavelengths followed similar trends. 440 nm was chosen because it contains the chlorophyll absorption peak. In October the mean attenuation coefficient at 440 nm in the middle of the Yellow Sea ranged from 0.18 m^{-1} to 1.08 m^{-1}. In June, it ranged from 0.37m^{-1} to 1.6 m^{-1}, in April from 0.7 to 1.6m^{-1}, and in February from 1.5 to 3.7 m^{-1}. Even the clearest areas of the Yellow Sea exhibited high attenuation coefficients. In coastal waters, attenuation coefficients were one and sometimes two orders of magnitude higher than those of the open waters. The overall minimum and maximum values of attenuation for all seasons are presented in Tables 1 and 2.

The area studied during this investigation was bound by 34°N and 37°N and by 124°E and 126°E. For analyses purposes, it was arbitrarily divided into a northern region (36°N to 37°N), a middle region (35°N to 36°N), and a southern region (34°N to 35°N). The southern coastal region located to the east of 125°E and off Mokpo was characterized by a strong and almost permanent particle resuspension which produced attenuation coefficients as high as 42.61 m^{-1} (at 440 nm). The extreme opacity of these waters challenged the limits of the instrumentation used. In the northern coastal area in front and south of Inchon high attenuation at 440 nm ranging from 1.84 m^{-1} to 2.0 m^{-1} were observed in October, 2.4 m^{-1} to 17 m^{-1} in April, and 4.0 m^{-1} to 30 m^{-1} in February. There was no data for June because of instrument failure during transects 307 and 308 of this cruise. The middle region was characterized by fairly clear waters during all seasons. Attenuation coefficients (at 440 nm) as low as 0.6 m^{-1} were recorded in October and as high as 4.2 m^{-1} in February. Isolated patches of high attenuation occurred during April ranging between 3.7 m^{-1} to 28.0 m^{-1}. These were probably the result of both sediment and phytoplankton spectral contributions.

Because of the shallow bathymetry, strong tides, and fine sediments, the optical field of Korean coastal waters exhibits a close relationship to the oceanographic and geological parameters of the area. The results of the statistical tests show correlation (R^2=0.48) between the spectral attenuation and the current speed. Further analyses and observation of the data indicated that it was not a single parameter, but rather a combination of parameters that determined the magnitude and maximum wavelength of the spectral attenuation in the proximity of the coast. For instance, a shifting from blue-green to yellow occurs during the ebb phase of the tide. Conversely,

Table 1. Minimum seasonal attenuation coefficients, C, at three wavelengths, and locations, and depths at which they occurred in the Yellow Sea

Season	Wave Length	C (m^{-1})	Lat (°N)	Long (°E)	Depth (m)	Station Number
June 96	440 nm	0.2982	34.72	124.60	9.5	311-09
	532 nm	0.2842	34.72	124.60	9.5	
	676 nm	0.6409	34.72	124.60	9.5	
October 96	440 nm	0.1873	35.85	124.38	55	309-10
	532 nm	0.1582	35.85	124.38	55	
	676 nm	0.5240	35.85	124.38	55	
April 98	440 nm	0.5185	35.90	125.00	27	309-7
	532 nm	0.4700	35.90	125.00	31	
	676 nm	0.7895	35.85	122.18	24	
February 99	440 nm	0.7399	35.85	125.41	4.75	309-5
	532 nm	0.6426	35.85	125.41	4	
	676 nm	0.9085	35.85	125.41	4.75	

Table 2. Maximum seasonal attenuation coefficients, C, at three wavelengths, and locations, and depths at which they occurred in the Korean coast of the Yellow Sea

Season	Wave Length	C (m^{-1})	Lat (°N)	Long (°E)	Depth (m)	Station Number
June 96	440 nm	29.4498	35.34	125.83	22	310-03
	532 nm	28.4032	35.34	125.83	22	
	676 nm	27.5796	35.34	125.83	22	
October 96	440 nm	31.6219	34.71	125.72	18	311-04
	532 nm	30.6050	34.71	125.72	18	
	676 nm	28.0122	34.71	125.72	18	
April 98	440 nm	38.0034	35.34	125.83	24.25	310-03
	532 nm	37.4328	35.34	125.83	24.25	
	676 nm	42.6129	35.34	125.83	22.75	
February 99	440 nm	41.0918	34.71	125.72	19.75	311-04
	532 nm	39.3978	34.71	125.72	19.5	
	676 nm	36.5877	34.71	125.72	19.75	

during the flood phase, the water is predominantly blue-green. The shifting in wavelength can be also observed in the remote sensing reflectance measured at two stations (Figs. 4a and 4b). These have the same meteorological conditions, bottoms and current speeds but opposite current directions. Fig. 4a was acquired when the current was flowing from the ocean towards the land. Its remote sensing reflectance shows a broad peak from 475 nm to approximately 550 nm. Conversely Fig. 4b depicts the remote sensing reflectance acquired over waters that were flowing from the land towards the ocean, with a very distinctive peak at 575 nm. Our data indicates that even a weak current can have substantial effects in the remote sensing reflectance if its direction is between 180° and 360° with respect to the Korean coastline. The changes in wavelength are a function of the resuspension of particles in the water column. During the ebb tide, the re-suspension is more apparent than during the flood stages, where clear water from offshore flows into the littoral areas.

Waters over silt bottoms had higher attenuation coefficients at 440 nm (>11 m^{-1}) than waters over sand bottoms (< 3.0 m^{-1}). This is attributed to the faster settling rate of the sand particles. Silt particles tend to remain in suspension longer, and in areas such those off Mokpo, never settle down completely. The type of bottom may explain the attenuation of the waters in the middle region of the coast, and the extreme high attenuations found in the southern region. In this area, stations 310-03, 311-04, and 311-05 had silt and clay bottoms and exhibited attenuations at 440 nm greater than 22 m^{-1}. Examples of various attenuation coefficients measured at 440 nm off the

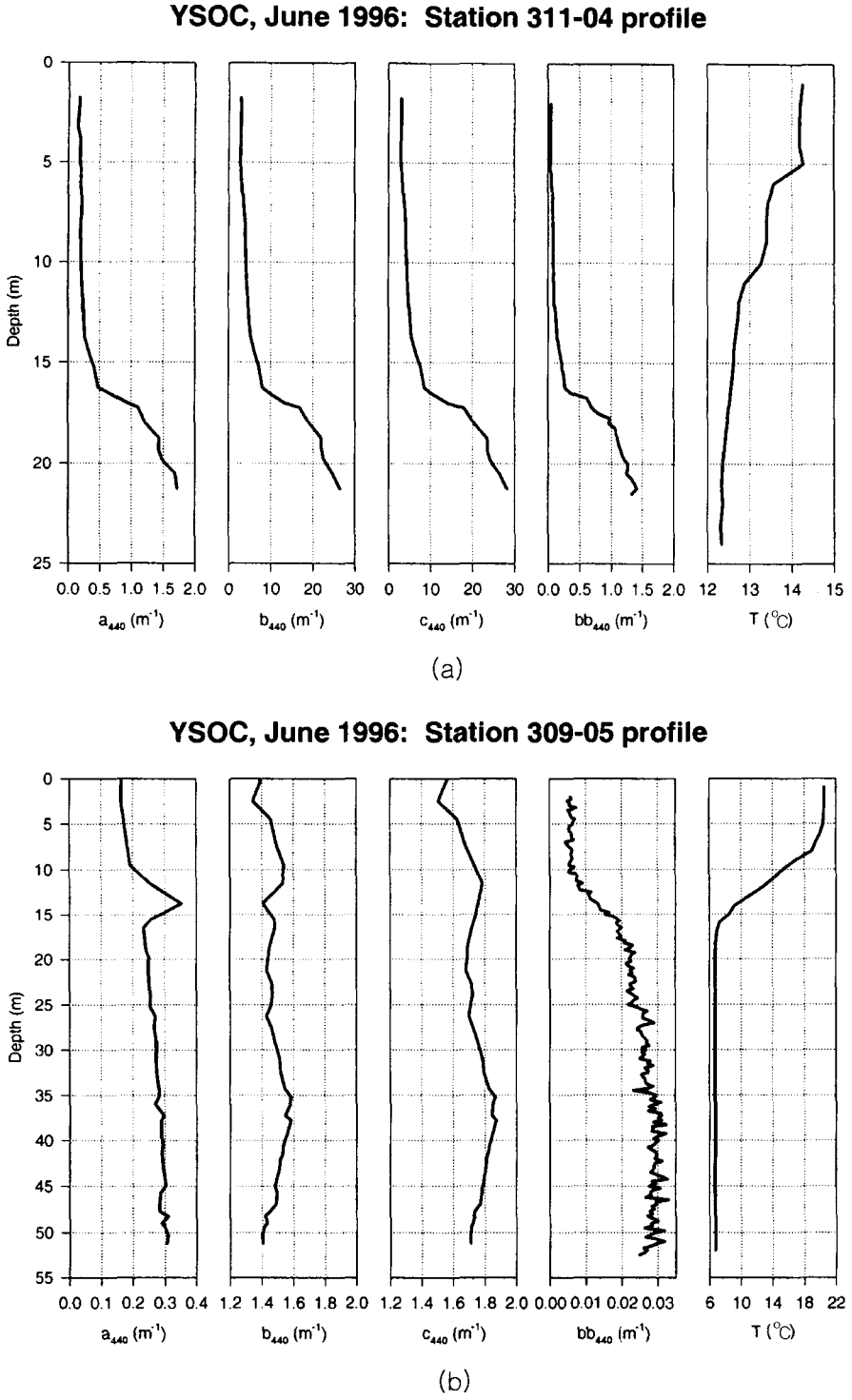

Fig. 4. Vertical distribution of optical parameters and temperature for a coastal and offshore stations.

coast of Korea, and the geological and parameters observed at the time of the measurements are presented below:

- High current speeds (>50 cm/s; 180° to 360°), silt bottoms, and shallow bathymetry (< 30 m).=41 m^{-1}
- Low currents (<11 cm/s; 180° to 360°) sandy bottoms and shallow bathymetry (<30 m).=38 m^{-1}
- Medium current speeds (>30 cm/s < 49 cm/sec; 1° to 180°), silt bottoms, and shallow bathymetry (<30 m).=32 m^{-1}
- High current speeds (>98 cm/s; 1° to 180°), sandy bottoms, and shallow bathymetry (<30 m)=29 m^{-1}
- Weak currents (<11 cm/s; 1° to 180°) sandy bot-

:oms and shallow bathymetry (<30 m).=< 2 m^{-1}

In summary, the lowest spectral attenuations of the :oastal stations were found in those stations that had weak currents directed towards the coast and which occurred over sand bottoms. The highest attenuations were found in areas with silt/clay bottoms which had strong tidal currents directed away from the coast.

There was no evidence in the analyzed data that :he current direction or speed were relevant or influ-:nced the optical measurements of the offshore sta-:ions (middle of the Yellow Sea). The factors that appear to control the offshore spectral attenuation are :he wind speed, phytoplankton blooms, and strati-fication of the water column. Sediment type is impor-:ant only in the deeper layers (10 m off the bettom). At high wind speeds, the spectral attenuation increases due to the increase in spectral scattering of particles and turbulent elements in the water. The high values of attenuation at 440 nm in the February data may be explained by the strong winds present during the sampling. Attenuation ranges of 0.30 m^{-1} to 2.96 m^{-1} at 440 nm were recorded at wind speeds of less than 50 cm/s at station 310-5 in October. Attenuation ranges of 2.30 m^{-1} to 7.30 m^{-1} were recorded at speeds of 150 cm/s in February at that same station. Besides these sporadic comparisons, it was not possible to conduct a full evaluation of the wind effect on the attenuation because our cruises were conducted for the most part under fair weather and low wind conditions.

Figs. 5a and 5b show measured profiles of temperature and attenuation. Fig. 5a depicts profiles representatives of the coastal waters. These are characterized by extremely high attenuation coefficients at the bottom, resulting from particles re-suspension by the stirring action of the tidal current. It is apparent from this figure that the optical profile and thermal profile do not have any common features. This is expected since these waters are completely mixed. Figure 5b depicts profiles representative of the open waters of the Yellow Sea. In this figure, decreases in temperature at 15 m coincide with increases in attenuation coefficients at 13 m. The decrease in temperature leads to changes in density. It is at these locations that the particles may become entrained leading to the observed increases in spectral attenuation. In general, the June, October and part of the April data showed increases in spectral attenuation between 13 m and 20 m in response to decreases in temperature in the open waters. In February, the water column appeared to be completely mixed and there were no increases in the attenuation in response to stratification. Teague *et al.* (1998) reported on the existence of three layers or flow regimes in the Yellow Sea. According to his data, the first layer is a sheer layer that extends from the surface to 22 m. The increases in spectral attenuation observed during these months occur between 13 and 20 m.

Patches of phytoplankton were found in discrete samples obtained in coastal and open waters of the Yellow Sea during the April 1998 cruise. Increases in spectral attenuation at all wavelengths were detected at all stations where the patches were found. In coastal waters, their spectral contribution was masked by the large quantities of sediment. Inspection of tables 1 and 2 show that both the minimum and maximum overall attenuations at 440 nm increased in April at all wavelengths studied. Further examination of the absorption and scattering data at 676 nm revealed that the absorption was greater than the scattering during April, indicating that the increase in attenuation may be a function of the phytoplankton pigment present in the measurements. The high val-

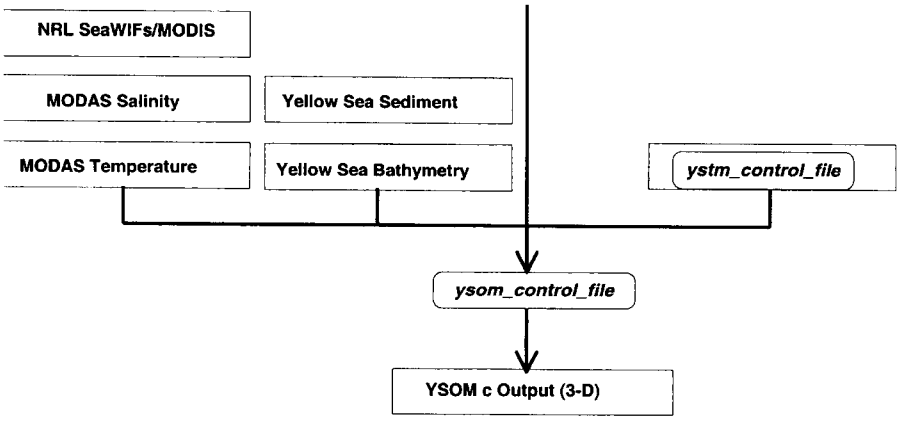

Fig. 5. Vertical distribution of temperature and attenuation coefficient for coastal (a) and offshore (b) stations.

ues in the red wavelengths occurred in the upper 29 meters in offshore waters that had silt bottoms, and in the upper 50 m in areas with sand bottoms. High values at 676 nm were also observed during the June 1996 cruise at 9 m and 23 m, indicating that blooms may also have been present during this time.

Waters west of 125.45°E exhibited low attenuation coefficients at 440 nm (<0.8 m^{-1}) throughout the seasons. Clear waters were found in October as deep as 55 m. In April, these waters extended to 30 m, in June to 10 m and in February to 5 m. Transect 309 had the largest number of stations with clear water, followed by transect 312. Minimum attenuation in both open and coastal waters was found in October and maximun attenuation in February. In April, increases in attenuation coefficient were measured at the surface in patches that exhibited high absorption coefficients.

VALIDATION AND MODEL RESULTS

For the evaluation of the YSOM, profiles of spectral attenuation coefficient computed by the model were compared with *in situ* profiles obtained during oceanographic campaigns in the Yellow Sea. The model was validated with an independent data set of *in situ* measurements which were not included in the training procedures. The accuracy with which the model estimated and reconstructed the *in situ* measurements was calculated with two basic statistical error measures conventionally used in model evaluation. These are Root Mean Square Error (RMSE) and Bias. However, because of the wide range in spectral attenuation at 532 nm (0.02 m^{-1} to 46.1 m^{-1}) in the Yellow Sea, a Normalized Root Mean Square Error (NRMSE) and Mean Absolute Percentage Error (MAPE) were also computed to normalize the error throughout the data. Table 3 shows the error in the model estimates at three different depths 0 m, 30 m and 60 m. The smaller errors occurred at the surface between 0 m and 5 m, and the larger errors were observed below 50 m. Comparisons between the model and the measurements (profiles) yielded RMSE of 0.19 m^{-1} at the surface, 0.41 m^{-1} at 30 m and 1.17 m^{-1} at 60 m; and MAPE of 2% at the surface 8% at 30 m and 15.8 % at 60 m. The increase in error with increase in depth resulted from the inclusion of the deep water data in the training procedures. A 60 m depth was arbitrarily set to train the neural network based on the area of re-suspension depicted by the satellite imagery. Since there was insufficient stations in waters shallower than 60 m to train the model, we included all the offshore station data from the surface to 60 m regardless of the bottom depth. After the model was trained and completed, we noted that in spite of having truncated the deeper portions of the data to 60 m, the model yielded excellent results for shallow water and satisfactory results for waters of the Yellow Sea which were deeper than 50 m. We expect to reduce the 15.8% error that occurs in the model estimation in waters deeper than 50 m by retraining the model using the full data sets. Attenuation in the open waters appears to be partly controlled by wind stress and localized phytoplankton blooms, neither of which is predictable. The inclusion of the satellite data may aid in the determination of phytoplankton concentrations. Wind is important in determining the spatial and temporal distribution of the spectral attenuation. The February estimates exhibited the highest level of error of all the months. This is also the windiest month of all the seasons sampled. The model currently operates at the NRL Ocean Optics Laboratory and computes data at five depths, 0 m, 5 m, 10 m 30 m and 60 m. An example of the spectral attenuation estimates produced by the model at the surface is presented in Fig. 6.

Table 3. Performance of the Yellow Sea Optical Model and average errors in its computations with respect to depth

Depth (m)	0	30	60
RMSE (m^{-1})	0.19	0.41	1.17
NRMSE (m^{-1})	0.56	0.73	0.79
BIAS (m^{-1})	0.05	0.13	0.55
MAPE (%)	2.10	8.40	15.8

CONCLUSIONS

The spectral attenuation in the Korean coastal waters of the Yellow Sea is two orders of magnitude higher than the attenuation observed in the offshore waters of the central Yellow Sea. It is highly controlled by the direction and speed of the current as well as by the type of bottom sediment. The highest values of spectral attenuation on the coast were associated with currents moving from inshore to offshore, which increased the attenuation as a result of the increase in particle number per unit volume. This contributes to the shifting of wavelengths from a blue-green to yellow observed in the remote sensing reflectance. The spectral attenuation of the offshore waters is influenced by the wind stress, phytopig-

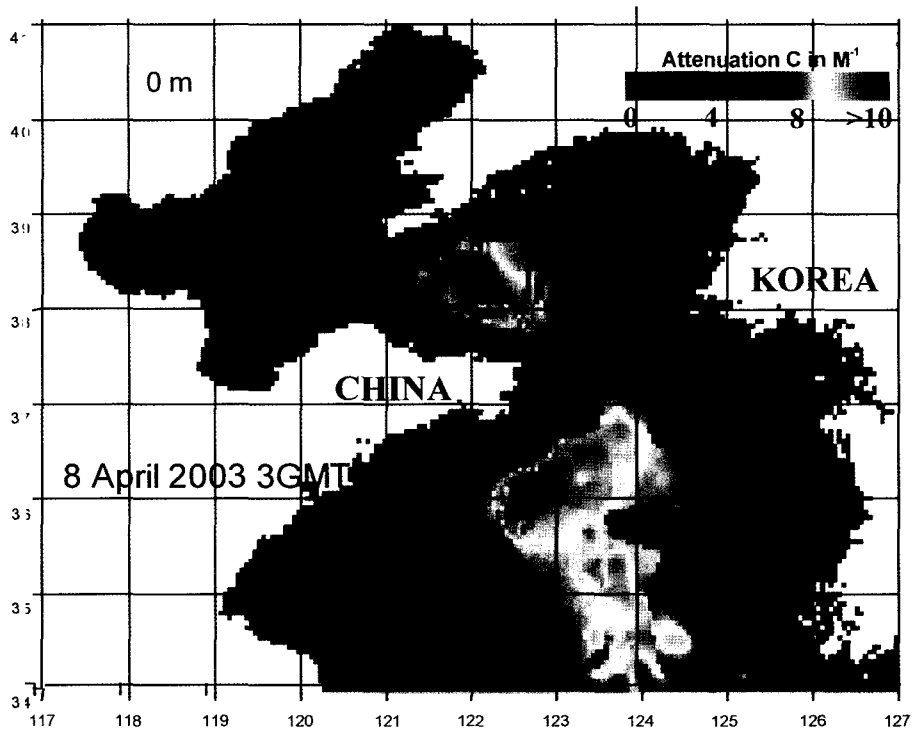

Fig. 6. A map of spectral attenuation estimates computed by the Yellow Sea Optical Model at the surface on 8 April 2003 at 3 GMT.

ments in the surface waters, and stratification of the water column. The type of sediment and current speed are important factors only in the lower 20 m. There is no evidence that the current speed or direction influenced the spectral attenuation of the offshore surface waters at any time during the course of this investigation. The highest spectral attenuation coefficients were observed in February and April and the lowest in October. June had relatively high spectral attenuation values (but not as high as those of February or April) at all stations and depths. Our findings corroborate previous findings by Hahn (1968), Choi and Shim (1986) and Ahn (1999).

Modeling of the spatio-temporal optical environment of the Yellow Sea using a physics-based approach is extremely complex and difficult. In this study we take a cause-effect approach to estimate the spatio-temporal distribution of the spectral attenuation. This approach was dictated by our findings of the linkages between the optical field to the local oceanographic and geological conditions. The result of our efforts is a neural network model based on a backpropagation learning algorithm that estimates spectral attenuation with respect to depth and time for the entire Yellow Sea relying mainly on its environmental conditions. The model was tested with data from the Korean coast and central Yellow Sea. Comparisons between the model and the measurements (profiles) indicated that the model is very accurate from the surface to a depth of 50 m. The error increases to 15.8% below this depth. The increase in error with increase in depth is attributed to the training procedures that did not include the entire length of the measured profile but that stopped at 60 m. There is evidence that accuracy of the model can be increased with the addition of wind data and data from other regions of the Yellow Sea. Although the amount of data increases the accuracy of neural network models, it is the variety of the data that allows the model to further generalize the estimates. Data from the coast of China are necessary to validate the model and possibly to improve its estimations.

The measurements and modeling of the spectral attenuation of the Yellow Sea illustrate the importance of real-time data for coastal waters. Satellite data provides synchronous and unparalleled views of the earth at least once a day, but their assessments and value are limited to the time of acquisition, exclusively. Extrapolating satellite data to other times of the day can introduce large errors to computations or estimations of the light field in the Yellow Sea coastal waters. The YSOM provides a realistic view of the spatio-temporal changes in spectral attenuation of the Yellow Sea. In contrast to the satellite data, the model can produce hourly real-time data not limited by cloud.

ACKNOWLEDGEMENTS

The authors would like to thank the scientists and staff of NFRDI and in particular those of the West Fishery Center, for providing support to this work. We are indebted to Captain Su Hwan Ku and the crew of the R/V Inchon 888 for their help during the cruises. We thank Ms. Cynthia Daniels of NRL-Oceanography Division for her help in running the neural network software and Mr. Chiu-Fu Cheng for optimizing the model and designing its graphics interface. This effort is the result of the close collaboration of Korean and American scientists. The Korean effort was supported by NFRDI. The American effort was supported by the office of the Oceanographer of the Navy (OP-096) and SPAWAR PMW 155: Program Element No. 0603207- Ocean Remote Sensing. Mr. Edward Harrison, Program Manager.

REFERENCES

Ahn, Y.H., 1999. Specific absorption coefficients for the chlorophyll and suspended sediment in the Yellow and Mediterranean Seas, J. Korean Soc. Remote Sens., **14**: 353–365.

Choi, B.H., 1988. A fine grid two-dimensional M2 tidal model of the East China Sea, J. Korean Assoc. Hydrol. Sci., **21**: 183–192.

Choi, J.K. and J.H. Shim, 1986. The ecological study of phytoplankton in Kyeonggi Bay, Yellow Sea. II Light intensity, transparency, suspended substances, J. Oceanol. Soc. Korea, **21**: 101–109.

Fei, Z., 1986. Study of the water color and transparency in the Bohai, J. Ocean. Huanghai and Bohai Seas, **4**: 33–40.

Fox, D.N., W.J. Teague, C.N. Barron, M.R. Carnes and C.M. Lee, 2002. The Modular Ocean Data Assimilation System (MODAS), J. Atmos. Ocean. Tech., **19**: 240–252.

Grabber, H.R.C. Beardsley and D. Grant, 1989. Storm generated surface waves in the East China Sea and the Yellow Sea, J. Phys. Ocean., **19**: 1039–1059.

Hu, D.X., 1994. Some striking features of the circulation in Huanghai Sea and East China Sea, Oceanology of the China Seas, **1**: 27–38.

Hanh, S.D., 1968. The relationship between the water color and the transparency in the seas around Korea, J. Ocean. Soc. Korea, **3**(2): 55–62.

Jacobs, G.A., R.H. Preller, S.K. Riedlinger, and W.J. Teague, 1998. Coastal wave generation in the Bohai Bay and propagation along the Chinese coast, Geophys. Res. Let. **25**: 777–780.

Kang, S.K., S.R. Lee and D.D. Yum, 1991. Tidal computation of the East China Sea, In *Oceanography of East and Asian Marginal Seas*, edited by A. Takano, pp. 25-48, Elsevier Pub., N.Y.

Milliman, J.D.F. Li, Y.Y. Shao, T.M. Zheng, and R. Limeburner, 1986. Suspended matter regime in the Yellow Sea, Prog. Oceanog. **17**: 215–227.

Pistek, P., H. Perkins and J. Boyd, 1998. Determining the Coastal Environment by data assimilation using an Adjoint technique, In *Rapid Environmental Assessment*, edited by Pouliquen, Kirwan and Pearson, pp. 35-41, NATO SACLANT Undersea Research Center, La Spezia, Italy.

Teague, W.J., H.T. Perkins, Z.R. Hallock, and G.A. Jacobs, 1998. Current and tide observations in the southern Yellow Sea, J. Geophys. Res., **103**: 27,783–27,793.

Wells, J.T., 1988. Distribution of suspended sediment in the Korea Strait and southeastern Yellow Sea: Onset of winter monsoons, Marine Geol., **83**: 273–284.

Yang, S., 1992. The light attenuation of the Euphotic zone in Qianliya waters in the middle of the Yellow Sea, Oceanol. Limnol. Sinica, **23**: 245–255.

Zhang, X., 1983. On the distribution characteristics of water transparency in the Each China Sea, Mar. Sci. Bull., **2**: 21–24.

Zhu, L. and B. Zhao, 1991. Distributions and variations of the transparency in the Bohai, Yellow Sea and East China Sea, Trans. Oceanol. Limnol., **3**: 1–11.

Manuscript received October 15, 2003
Revision accepted February 15, 2004
Editorial handling: Tetsuo Yanagi